Stripe width and nonlocal domain walls in the two-dimensional dipolar frustrated Ising ferromagnet

Alessandro Vindigni,[1] Niculin Saratz,[1] Oliver Portmann,[1] Danilo Pescia,[1] and Paolo Politi[2]
[1]*Laboratorium für Festkörperphysik, Eidgenössische Technische Hochschule Zürich, CH-8093 Zürich, Switzerland*
[2]*Istituto dei Sistemi Complessi, Consiglio Nazionale delle Ricerche, Via Madonna del Piano 10, 50019 Sesto Fiorentino, Italy*
(Received 21 February 2008; published 28 March 2008)

We describe a type of magnetic domain wall that, in contrast to Bloch or Néel walls, is nonlocalized and, in a certain temperature range, nonmonotonic. The wall appears as a mean-field solution of the two-dimensional ferromagnetic Ising model frustrated by a long-ranged dipolar interaction. We provide experimental evidence of this wall delocalization in the stripe-domain phase of perpendicularly magnetized ultrathin magnetic films. In agreement with experimental results, we find that the stripe width decreases with increasing temperature and approaches a finite value at the Curie temperature following a power law. The same kind of wall and a similar temperature dependence of the stripe width are expected in the mean-field approximation of the two-dimensional Coulomb frustrated Ising ferromagnet.

DOI: 10.1103/PhysRevB.77.092414 PACS number(s): 75.60.Ch, 05.70.Fh, 64.60.Cn

I. INTRODUCTION

Recent rigorous works[1,2] state that the spontaneous magnetization of a two-dimensional (2D) Ising ferromagnet exactly vanishes if a dipolar coupling is present [dipolar frustrated Ising ferromagnet (DFIF)]. Frustrating interactions on different spatial scales occur, e.g., in ultrathin magnetic films where the spins point perpendicular to the film plane.[1,3–14] Several approaches indicate a striped ground state[1,3,6,15,16] with spin modulation along one in-plane direction and a uniform spin alignment along the orthogonal in-plane direction. At finite temperatures, such spin "microemulsions"[17] suffer from the Landau–Peierls instability[1,5,9–14] that delocalizes the stripe position in the thermodynamic limit, thus reducing the positional order to a quasi-long-range one.[2,5,9] Notice, however, that the stripe width remains well defined at finite temperatures even in the thermodynamic limit[18] and that experiments on real systems do, indeed, observe the persistence of stripe order at finite temperatures,[4,7,11,12,19] possibly because of domain-wall pinning.[9,20,21] It is thus worthwhile to study the mean-field (MF) behavior of a DFIF at finite temperatures in the hope that some characteristics are "robust" enough to be valid beyond the MF approximation and to be observable in experiments. Competing interactions acting on different length scales are fundamental to many different chemical and physical systems[4,22–25] so that robust MF results on such a general model such as the DFIF may have a wide significance.

A central question that motivated this work is the equilibrium stripe width h^* (number of lattice parameters) at finite temperatures. One result appears to be well established in two dimensions: The stripe width in the ground state depends exponentially on the ratio between the exchange (J) and the dipolar (g) energy per atom.[1,8,9,16,17] The stripe width's temperature dependence, on the other hand, is controversial. Within the MF approximation, h^* is expected to decrease with temperature because it reaches a finite value on the order of $\frac{J}{g}$ at the temperature T_c of the MF transition to the paramagnetic state where the spin averages to zero at every site.[8,15] Theoretical arguments based on sharp interfaces[26–28] predict a (stretched) exponential decrease in $h^*(T)$ down to an atomic length scale at the transition temperature T_c. Within the spherical approximation, the modulation length of a related model (the Coulomb frustrated ferromagnet) "monotonically increases with temperature until it diverges at a disorder line temperature," and this is found regardless of the dimensionality of the system.[29] Experimental results on the temperature dependence of the stripe width are controversial as well,[12,19,24] and, in some cases, experiments do not show any change in h^* with temperature.[4]

In spite of its apparent simplicity, a detailed study of the stripe width of a DFIF as a function of temperature within the MF approximation has not been reported yet. Here, we fill this gap and solve the relevant MF equations for the DFIF model on a discrete lattice. We find a number of unexpected results. (1) The sharp-interface assumption gives correct stripe widths at low temperatures but fails to reproduce the results of the full MF calculation close to the transition temperature T_c. (2) Near T_c, the temperature dependence of h^* crosses over to a power law. (3) This crossover is accompanied by a delocalization of the wall between adjacent stripes. The profile changes from squarelike at low temperatures to cosinelike at T_c. (4) At intermediate temperatures, the interface between two adjacent stripes develops a pronounced nonmonotonic "shoulder" tailing down toward the center of the stripes according to a power law. The profile of these nonlocal walls is in striking contrast to that of the domain walls encountered in the Ising model without a dipolar interaction.[30] Their shape is also different from the shape of conventional Bloch or Néel walls that divide domains in typical Heisenberg or planar ferromagnets.[31] The strength of the shoulder structure at intermediate temperatures depends on the relative strength of J and g, but it occurs over mesoscopic scales and in a sizeable range of temperatures so that it should become observable by using spatially resolved experiments that have a high enough signal-to-noise ratio. The cosinelike profile, on the other hand, is observed sufficiently close to T_c independent of the ratio $\frac{g}{J}$. Here, we provide experimental evidence that the spin profile of the stripes changes, indeed, from squarelike at low temperatures to cosinelike at T_c.

 ©2008 The American Physical Society

II. MODEL

The DFIF Hamiltonian on a discrete lattice reads $\mathcal{H}=-\frac{J}{2}\sum_{\langle i,j\rangle}^{N}\sigma_i\sigma_j+\frac{g}{2}\sum_{\{i\neq j\}}^{N}\frac{\sigma_i\sigma_j}{|\vec{r}_{ij}|^3}$, where i and j are two-dimensional indices $[i\equiv(i_x,i_y)]$, with $1\leq i_x\leq L_x$ and $1\leq i_y\leq L_y$, $\sigma_i=\pm 1$, $\langle i,j\rangle$ means that the sum is restricted to nearest neighbors, $\{i\neq j\}$ indicates a sum over all the different pairs in the lattice, and $N=L_xL_y$ is the total number of spins. This system is treated in the MF approximation, and the spin superstructure is assumed to be a striped pattern (a very common pattern in real systems), i.e., we require the averages $m_{(i_x,i_y)}\doteq\langle\sigma_{(i_x,i_y)}\rangle$ to be translationally invariant along the y direction and periodic along the x direction with a period of $2h$: $m_{(i_x,i_y)}\equiv m_{i_x}$ and $m_{i_x+\alpha h}\equiv(-1)^{\alpha}m_{i_x}$, where $\alpha\in\mathbb{Z}$. The relevant MF quantities are thus reduced to the h independent variables m_{i_x}. To determine the equilibrium configurations, we first find the profile for a given h from the self-consistent MF equations $m_{i_x}=\tanh(\beta\Sigma_{j_x}V^h_{i_x,j_x}m_{j_x})$, where $\beta=1/k_BT$ and $V^h_{i_x,j_x}$ is the effective interaction matrix.[32] Then, we minimize the free energy per spin,

$$F^h=\frac{1}{2h}\sum_{i_x=1}^{h}\sum_{j_x=1}^{h}V^h_{i_x,j_x}m_{i_x}m_{j_x}-\frac{1}{h}\beta^{-1}\sum_{i_x=1}^{h}\ln\left[2\cosh\left(\beta\sum_{j_x=1}^{h}V^h_{i_x,j_x}m_{j_x}\right)\right],$$

with respect to h.

III. STRIPE WIDTH

Typically, in thin magnetic films, $J\gg g$. We are thus interested in large ratios $\delta\equiv J/g$, for which we recover the value of $h^*(T=0)$ known from Ref. 16 and the finite value $h^*(T_c)$ known from Ref. 8. T_c and the limiting magnetization profile $m_{i_x}(T\to T_c)$ [see Fig. 2(a)] are found as the maximum eigenvalue and the corresponding eigenvector of $V^h_{i_x,j_x}$.[33] In Fig. 1, we plot $h^*(T)$ for $\delta=10$. The polygonal appearance of the graphs is due to h^* changing only by ±1 in a discrete model. In order to understand the low-temperature behavior of $h^*(T)$ and the low-T plateau, we introduce a manageable "sharp-interface" two-spin model, where $m_1=m_h\equiv m_w$ and $m_{i_x}\equiv m_b$ for $i_x\neq 1,h$ (lower left inset in Fig. 1). In the limit of large δ, m_b is just the MF value for a ferromagnetic Ising model, $m_b=\tanh(4\beta Jm_b)$, and m_w is the corresponding MF value for a spin adjacent to a domain wall, i.e., $m_w=\tanh[\beta J(m_w+m_b)]$. Due to the reduced exchange energy in the argument of the tanh, $m_w(T)\leq m_b(T)$ [see Fig. 2(a)]. By inserting $m_w(T)$ and $m_b(T)$ into the sharp-interface free energy and minimizing it with respect to h, we obtain $h^*_{2\text{spin}}(T)=\exp(1+A/4gm_b^2)$, where $A=J(m_w^2+m_wm_b-4m_b^2)-k_BT\ln[(1-m_b^2)/(1-m_w^2)]$. The dashed curve in Fig. 1, which represents $h^*_{2\text{spin}}(T)$ for $\delta=10$, reproduces the low-temperature behavior of the numerical solution but fails at higher temperatures, where it gives $h^*_{2\text{spin}}(T_c)\approx1$. In the upper inset in Fig. 1, we plot $h^*(T)-h^*(T_c)$ vs $(T_c-T)/T_c$ for the full MF calculation close to T_c in a log-log plot, showing that the domain width asymptotically behaves according to a power law $h^*(T)-h^*(T_c)\sim(T_c-T)^{\lambda}$, with $\lambda\approx2$, as discussed in the figure caption. This numerical outcome seems to confirm the conjecture of Ref. 19 but is at odds with the sharp-interface limit of Refs. 26–28. It would be interesting to review the experimental results of Refs. 12 and 24 under the point of view of a power law. The argument of Ref. 19 associates the crossover to a power-law behavior with higher harmonics (responsible for the sharp interface at low temperatures) that vanish with increasing temperature and, thus, with the broadening of the spin profile to a cosinelike profile close to T_c.

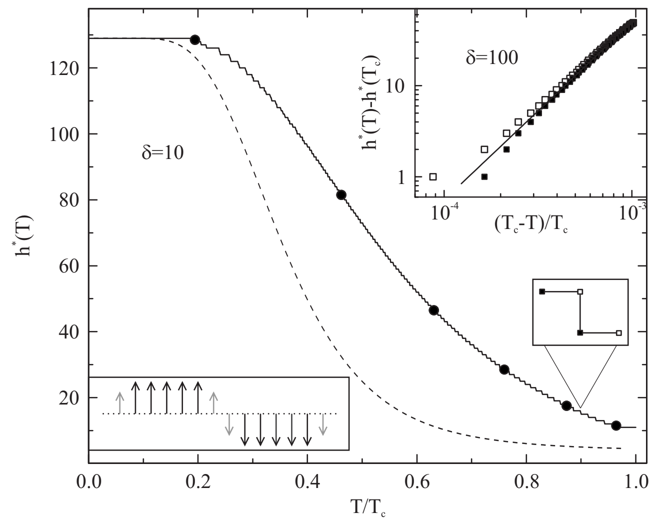

FIG. 1. Equilibrium stripe width. The solid line represents $h^*(T)$ as a function of the reduced temperature T/T_C for $\delta=10$. The dots on the line are those points for which we show spin profiles in Fig. 2(a). The upper inset plots $h^*(T)-h^*(T_c)$ versus $(T_c-T)/T_c$ in the critical region for $\delta=100$. Full (empty) dots correspond to the upper (lower) corners of the steps of the $h^*(T)$ curve (see sketch, lower right). A fit to the full dots is shown. The fit of the full (empty) dots gives an exponent of 2.0 (1.9). The dashed line shows $h^*_{2\text{spin}}(T)$, which is calculated within the two-spin model (sharp-interface limit) for $\delta=10$. The lower left inset illustrates the two-spin model.

IV. MAGNETIZATION PROFILE

The spin profiles m_{i_x} at different temperatures, which are obtained from the transcendental MF equations, are plotted in Fig. 2(a) for selected temperatures (marked with dots in Fig. 1). We identify three regimes: (i) First is a low-T regime with a squarelike profile that corresponds to the plateau in the $h^*(T)$ curves. (ii) Second is an intermediate T regime that corresponds to the steep descent of $h^*(T)$. Here, features including a double shoulder and a wall delocalization are observed. (iii) Third is a high-T regime that corresponds to the critical region, where magnetization has, indeed, a cosinelike profile, which is also expected from analytical considerations and leads to the power-law behavior of the equilibrium stripe width.[19] Notice that the interface is sharp within the first regime and the bulk magnetization $m_2,\ldots,m_{h-1}$ (circles) does not change very much, which justifies the two-spin model (dashed curve in Fig. 1). In order to understand the

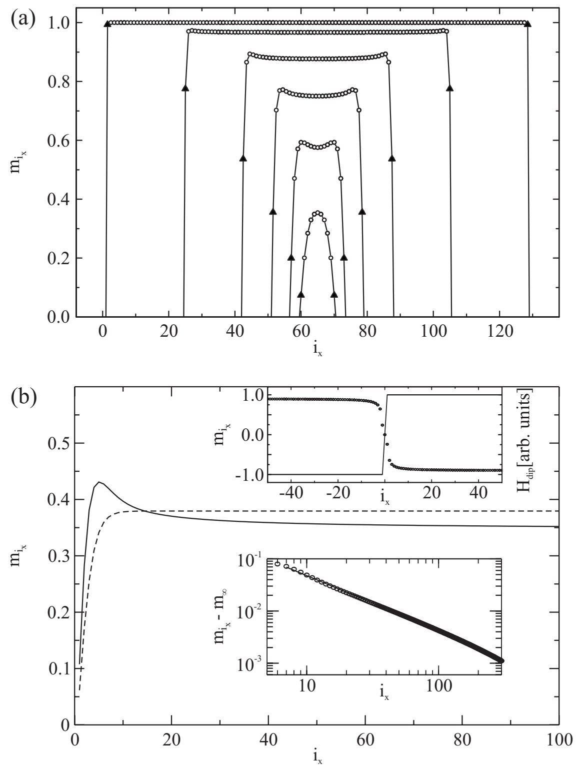

FIG. 2. (a) Spin profile within a stripe calculated for $\delta=10$ at different temperatures and the corresponding values of $h^*(T)$. The triangles locate the interface spins. (b) Spin profile for a single domain wall with $\delta=10$ (solid line) and $\delta=\infty$ (Landau profile, dashed line) for $T/T_C=0.95$. The magnetization exponentially approaches the $m(\infty)$ value for $\delta=\infty$, but it decays as $1/i_x$ for finite δ (lower inset). The upper inset shows the demagnetizing field (dots) that originates from the dipolar interaction for a steplike spin profile (solid line).

origin of the nonmonotonic shoulder and the wall delocalization, we have solved the MF equations for a single domain wall. In Fig. 2(b), we compare the profiles in the absence (dashed line) and in the presence (solid line) of a dipolar interaction. For $\delta=\infty$ ($g=0$), the profile is a Landau type one. It monotonically increases and exponentially attains the asymptotic value. For finite δ, the profile is not monotonic. It has a shoulder close to the wall center and then decays to $m(+\infty)$ as the inverse of the distance (lower inset). Both features derive from the dipolar (demagnetizing) field $H^{\mathrm{dip}}(i_x)$, which is plotted for a steplike profile in the upper inset. Close to the center of the wall, $H^{\mathrm{dip}}(i_x)$ almost vanishes because of the compensation between the fields generated by up and down spins. There, the deviation from the Landau-type wall (dashed line) is small. The approach to the $H^{\mathrm{dip}}(+\infty)$ value occurs as $1/i_x$ and depresses the spin profile below the asymptotic value for $g=0$. We have also checked within a continuum model that the demagnetizing field far from the wall vanishes in the infinite-thickness limit so that the three-dimensional, monotonic, and localized "Landau" wall is recovered in three dimensions. Thus, the formation of the nonmonotonic long-ranged wall is a purely two-dimensional effect.

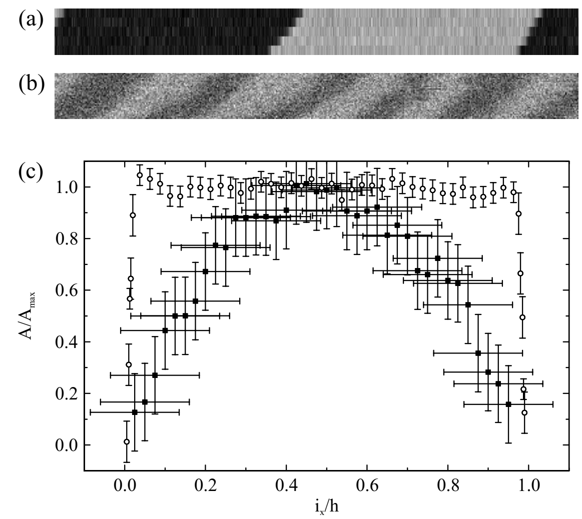

FIG. 3. (a) SEMPA (Refs. 19 and 34) measurement of a stripe section at low temperature (10 K). The spin polarization is encoded by a gray scale. The measured image is 4000 pixels (17 μm) wide and 5 pixels (21 nm) high. For a better inspection, the image has been stretched by a factor of 70 along the vertical direction. Within the spatial resolution of the experiment, this mesurement corresponds to five scans of the same scan line, which are displayed as successive lines in one image. Thermal drift causes some displacement between the scan lines. (b) SEMPA measurement of a stripe section at a high temperature (330 K). The measured image is 400 pixels (4.25 μm) wide and 35 pixels (370 nm) high. This image is displayed in its real proportions. (c) Experimental spin profiles across one stripe at a low temperature (10 K, $h=9$ μm, empty circles) and close to the transition temperature (330 K, h =430 nm, black squares), as extracted from images (a) and (b), respectively. To obtain the profile, the scan lines are aligned to compensate for the thermal drift. Then, the aligned scan lines are averaged. To further reduce the noise level, these raw profiles are resampled by averaging a number of adjacent points. Both profiles have been normalized to the same width and amplitude. The horizontal error bars represent the spatial resolution (± 50 nm) of the experiment. It is determined from the topographic profile of a sharp edge, which is obtained by the same procedure from a topographic image measured with exactly the same parameters as the magnetic image in (b). For the low-T profile, the horizontal error is on the order of the size of the data points. The vertical error bars are due to the statistical noise of the secondary electrons counted in SEMPA (Refs. 19 and 34). Note that no traces of an in-plane component of the spin polarization can be found in simultaneously recorded images of the in-plane spin polarization. Details of the experiment will be published in a more extended review and are available on request.

The squarelike profile at low temperatures delocalizes into a cosinelike profile close to T_c, no matter how small the dipolar interaction is. We provide experimental evidence of this wall delocalization in Fig. 3. The spin profile was measured in SEMPA[19] experiments on ultrathin Fe films epitaxially grown on Cu(100). These systems are magnetized perpendicular to the film plane and show the sought-for stripe structure.[34] The two different profiles at low temperatures (empty dots) and close to the stripe-paramagnetic transition temperature (full dots) point to the realization of the MF crossover shown in Fig. 2(a).

V. CONCLUSIONS

In summary, we have shown that when dealing with "spin microemulsions" (and probably with analogous pattern-forming systems), the range of validity of a sharp-interface limit must be carefully evaluated and that important physical features, such as the stripe width, crucially depend on whether the actual interface is sharp or not. In addition, we have discovered that Landau-type walls (and, probably, Bloch- and Néel-type walls as well) must be modified in low-dimensional systems because a dipolar interaction produces a nonmonotonic long-ranged tail, which is absent in three-dimensional systems, such as those considered by Landau.[31] Our study has focused on the DFIF model on a discrete lattice. However, our results appear to be relevant[35] for Coulomb frustrated Ising ferromagnets[36] as well. In the Coulomb system, antiferromagnetic interactions decay as $|\vec{r}|^{-1}$ rather than as $|\vec{r}|^{-3}$, like the dipolar interaction, but preliminary results indicate that the phenomenology (domain shrinking, power-law approach to a finite value at T_c, delocalization, and presence of a shoulder in the domain-wall profile) is the same. Although our work is based on the MF approximation, it produces results that appear to be realized in real pattern-forming systems, such as the power-law dependence of the stripe width[19] and the spin profile [Fig. 3(c)], and it might provide a reasonable starting point for more sophisticated theoretical works.

ACKNOWLEDGMENTS

We acknowledge financial support by ETHZ and the Swiss National Science Foundation and fruitful discussions with S. A. Cannas, E. Tosatti, G. E. Santoro, and Z. Nussinov.

[1] A. Giuliani, J. L. Lebowitz, and E. H. Lieb, Phys. Rev. B **74**, 064420 (2006).

[2] M. Biskup, L. Chayes, and S. A. Kivelson, Commun. Math. Phys. **274**, 217 (2007).

[3] C. Kooy and U. Enz, Philips Res. Rep. **15**, 7 (1960).

[4] M. Seul and D. Andelman, Science **267**, 476 (1995), and references therein.

[5] T. Garel and S. Doniach, Phys. Rev. B **26**, 325 (1982).

[6] Kwok-On Ng and D. Vanderbilt, Phys. Rev. B **52**, 2177 (1995).

[7] D. Sornette, J. Phys. France **48**, 151 (1987), and references therein.

[8] R. Czech and J. Villain, J. Phys.: Condens. Matter **1**, 619 (1989).

[9] A. B. Kashuba and V. L. Pokrovsky, Phys. Rev. B **48**, 10335 (1993); Ar. Abanov, V. Kalatsky, V. L. Pokrovsky, and W. M. Saslow, *ibid.* **51**, 1023 (1995).

[10] K. De'Bell, A. B. MacIsaac, and J. P. Whitehead, Rev. Mod. Phys. **72**, 225 (2000); S. A. Cannas, D. A. Stariolo, and F. A. Tamarit, Phys. Rev. B **69**, 092409 (2004), and references therein.

[11] R. Allenspach and A. Bischof, Phys. Rev. Lett. **69**, 3385 (1992).

[12] C. Won, Y. Z. Wu, J. Choi, W. Kim, A. Scholl, A. Doran, T. Owens, J. Wu, X. F. Jin, H. W. Zhao, and Z. Q. Qiu, Phys. Rev. B **71**, 224429 (2005).

[13] C. B. Muratov, Phys. Rev. E **66**, 066108 (2002).

[14] A. D. Stoycheva and S. J. Singer, Phys. Rev. Lett. **84**, 4657 (2000).

[15] J. Castro, G. A. Gehring, and S. J. Robinson, J. Magn. Magn. Mater. **214**, 85 (2000).

[16] A. B. MacIsaac, J. P. Whitehead, M. C. Robinson, and K. De'Bell, Phys. Rev. B **51**, 16033 (1995).

[17] R. Jamei, S. Kivelson, and B. Spivak, Phys. Rev. Lett. **94**, 056805 (2005).

[18] B. Jancovici, Phys. Rev. Lett. **19**, 20 (1967).

[19] O. Portmann, A. Vaterlaus, and D. Pescia, Phys. Rev. Lett. **96**, 047212 (2006), and references therein.

[20] In Fe films on Cu(100), the coercive field, which is a measure of the barrier for a domain-wall motion, is found to be small but finite.

[21] S. Lemerle, J. Ferré, C. Chappert, V. Mathet, T. Giamarchi, and P. Le Doussal, Phys. Rev. Lett. **80**, 849 (1998).

[22] D. Andelman, F. Brochard, and J.-F. Joanny, Proc. Natl. Acad. Sci. U.S.A. **84**, 4717 (1987).

[23] P. Ball, *The Self-Made Tapestry: Pattern Fomation in Nature* (Oxford University Press, Oxford, 2001).

[24] S. L. Keller and H. M. McConnell, Phys. Rev. Lett. **82**, 1602 (1999), and references therein.

[25] F. S. Bates and G. H. Fredrickson, Phys. Today **52**(2), 32 (1999).

[26] G. A. Gehring and M. Keskin, J. Phys.: Condens. Matter **5**, L581 (1993).

[27] H. M. McConnell, Annu. Rev. Phys. Chem. **42**, 171 (1991).

[28] A. D. Stoycheva and S. J. Singer, Phys. Rev. E **64**, 016118 (2001).

[29] Z. Nussinov, J. Rudnick, S. A. Kivelson, and L. N. Chayes, Phys. Rev. Lett. **83**, 472 (1999); Z. Nussinov, arXiv:cond-mat/0506554 (unpublished).

[30] E. Ising, Zh. Eksp. Teor. Fiz. **31**, 253 (1925).

[31] L. D. Landau, in *Collected Papers*, edited by D. Ter Haar (Gordon and Breach, New York, 1967), pp. 101–116; A. Hubert and R. Schäfer, *Magnetic Domains* (Spinger, Berlin, 2000).

[32] The effective interaction is given by $V^h_{i_x,j_x}=J\Delta_{i_x,j_x}-g\Gamma_{i_x,j_x}$, where Δ_{i_x,j_x} accounts for the number and relative orientation of spins in column j_x, which are nearest neighbors of a single spin in column i_x: $\Delta_{i_x,i_x}=2$, $\Delta_{i_x,i_x\pm 1}=1(i_x\neq 1,h)$, $\Delta_{1,h}=\Delta_{h,1}=-1$, and $\Delta_{i_x,j_x}=0$ otherwise. $\Gamma_{i_x,j_x}=\Sigma_\alpha\Sigma_{j_y=1}^{L_y}\frac{(-1)^\alpha}{|(j_x-i_x+\alpha h)^2+(j_y-1)^2|^{3/2}}$, where the term for $\alpha=0$ has to be omitted for $i_x=j_x$.

[33] The MF solution $\underline{m}\equiv(m_1,\ldots,m_h)$ fulfills the condition $|\underline{m}|^2\leq\frac{1}{T^2}|V^h\underline{m}|^2$ and can be written in the basis of the eigenvectors $\underline{m}_\mu$ of V^h with eigenvalues λ_μ as $\underline{m}=\Sigma_\mu a_\mu\underline{m}_\mu$. Then, $\Sigma_\mu a_\mu^2\leq\Sigma_\mu(\frac{\lambda_\mu}{T})^2a_\mu^2$. For $T>T_c=\lambda_{\max}$, the only solution is $a_\mu^2=0\ \forall\mu$.

[34] O. Portmann, A. Vaterlaus, and D. Pescia, Nature (London) **422**, 701 (2003).

[35] O. Portmann and D. Pescia (unpublished).

[36] P. Viot and G. Tarjus, Europhys. Lett. **44**, 423 (1998).